Experimental Evaluation of Robot-Assisted Tactile Sensing for Minimally Invasive Surgery

Ana Luisa Trejos, Jagadeesan Jayender, *Member, IEEE*, Melissa T. Perri, Michael D. Naish, *Member, IEEE*, Rajni V. Patel, *Fellow, IEEE,* and Richard A. Malthaner

***Abstract*—The 10 mm incisions used in minimally invasive cancer surgery prevent direct manual palpation of internal organs, making intraoperative tumor localization difficult. A tactile sensing instrument (TSI), that uses a commercially available sensor to measure distributed pressure profiles along the contacting surface, has been developed to facilitate remote tissue palpation. The objective of this research was to assess the feasibility of using the TSI under robotic control to reliably locate underlying tumors. The performance of human and robot manipulation of the TSI to locate tumor phantoms embedded into *ex vivo* bovine livers was compared. An Augmented Hybrid Impedance Control scheme was implemented on a Mitsubishi PA10-7C robot to perform force/position control during the trials. The results showed that using the TSI under robotic control realized an average 35% decrease in the maximum forces applied, and more than a 50% increase in tumor detection accuracy when compared to manual manipulation of the same instrument. This demonstrates that tumor detection using tactile sensing is highly dependent on the consistent application of forces on the tactile sensing area and that robotic assistance can be of great benefit when trying to localize tumors during minimally invasive surgery.**

I. Introduction

CANCER is the second leading cause of death in North America and Europe [1]. Once diagnosed, surgical resection of the tumor is the treatment of choice to prevent the spread of cancer. Imaging techniques such as MRI or CT scanning are critical for identifying the presence of lesions pre-operatively; however, intraoperatively, the surgeon often relies on direct manual palpation of the tissue to confirm tumor location. Malignant tumors are commonly stiffer than the surrounding tissue, allowing them to be easily identified as hard nodules when palpated [2].

Traditional tumor resection surgery involves accessing the diseased tissue through a large incision in the chest or abdominal wall, leading to a highly invasive procedure. Increasingly, surgical procedures are being performed through 10 mm incisions using long, narrow instruments. These minimally invasive approaches offer the advantages of reduced tissue trauma, decreased risk of infection, faster recovery time and reduced associated costs.

During surgery, the position of a tumor differs from that in a preoperative scan due to tissue shift and, in the case of lung cancer surgery, collapsing of the lung. In minimally invasive surgery (MIS), tissue shift is aggravated by insufflation of the abdomen or chest. Furthermore, direct manual palpation of the tissue is not possible due to the size of the incision. Instead, MIS instruments must be used to probe the tissue. The surgeon's ability to use these instruments for force feedback is compromised by friction and moments introduced by the trocar and the cavity wall. MIS ultrasound is an alternative method that is not dependent on kinesthetic feedback and is commonly used for tumor identification; however, it is not always available and its performance, particularly in the lung, is greatly limited.

In view of these limitations, an alternative method for locating tumors is required to improve the likelihood that a tumor resection can be completed using minimally invasive techniques. One such method, which has been the subject of considerable research, is the relay of haptic cues from tissue-instrument interaction to the user interface. Haptic information can be considered in two distinct modes: kinesthetic and tactile [3]. This work focuses on tactile sensing, which includes the sensation of surface textures, or distributed pressures acting across the contacting surface. The measurement of tactile information requires a tightly packed array of sensors capable of measuring multiple contact pressures or forces concurrently.

A. Passive Measurement

A variety of hand-held instruments have been developed to measure tissue interaction forces. Examples of instrumented graspers can be found in [2,4,5]. A 2D mechanical sensor capable of measuring thrust and pull inside instrument jaws is proposed in [6]. Other researchers, such as [7,8] have tried sensing the forces on the handle of the instrument. Reference [9] proposes the use of a novel

Manuscript received April 23, 2008. This research was supported by the Natural Sciences and Engineering Research Council (NSERC) of Canada under grants RGPIN-1345 (R.V. Patel), and 312383-2005 (M.D. Naish); by the Ontario Research and Development Challenge Fund under grant 00-May-0709 (R.V. Patel); and by infrastructure grants from the Canada Foundation for Innovation awarded to the London Health Sciences Centre (Canadian Surgical Technologies & Advanced Robotics (CSTAR)) and to The University of Western Ontario (UWO) (R.V. Patel).

A.L. Trejos, J. Jayender, and M.T. Perri are with CSTAR, Lawson Health Research Institute, 339 Windermere Road, London, ON, Canada and with the Department of Electrical and Computer Engineering, UWO, London, ON, Canada (phone: 519-685-8500 ext. 32529, email: analuisa.trejos@lhsc.on.ca, jjagadee@uwo.ca, mperri3@uwo.ca).

R.V. Patel is with CSTAR, the Department of Electrical and Computer Engineering and the Department of Surgery, UWO, (email: rajni.patel@lhsc.on.ca).

M.D. Naish is with CSTAR, the Department of Mechanical and Materials Engineering, and the Department of Electrical and Computer Engineering, UWO, (email: naish@eng.uwo.ca).

R.A. Malthaner is with CSTAR and the Dept. of Surgery, Division of Thoracic Surgery, UWO, (email: richard.malthaner@lhsc.on.ca).

high-accuracy 3-degree-of-freedom (DOF) miniature force sensor to measure tip forces.

An instrumented grasper was used to locate artificial tumors implanted in porcine bowel in [10]. While effective, it was found to be significantly slower than both direct palpation and the use of a standard instrument. Tactile feedback systems have also been proposed for identification and characterization of lesions in the breast [11] and for identifying arteries during robotic surgery [12]. The use of tactile sensors to identify pulmonary lesions using a capacitive array was discussed in [13]. Validation tests using a foam model showed promising results.

B. Active and Robotic Measurement

Some of the difficulties encountered during MIS due to reduced access conditions have been solved by the use of robotic systems. In master-slave systems, the surgeon remotely controls the instruments, while a slave robot mimics the surgeon's motions and performs the procedure. Reversal of hand motion, force magnification, and poor dexterity are eliminated, while hand tremors are filtered and the view of the surgical field is magnified. Unfortunately, these systems are unable to accurately transfer interaction forces between the tissue and the instrument tip to the surgeon.

A number of master-slave systems, capable of providing haptic feedback and suitable for the evaluation of tissue stiffness through kinesthetic sensing have been developed, e.g., [14, 15]. The system developed in [16] employs a robot to automatically palpate for a patient's arterial pulse at the wrist. While not suitable for MIS procedures, this system stands out as the only automated system to use tactile sensing for diagnostic purposes. Research presented in [17] evaluates the effect of using a master-slave robotic system equipped with tactile sensing capabilities for tumor detection. Feedback to the user is provided via a tactile display. The results showed that the performance of the system was greatly dependent on how well the exploration force could be controlled by the user.

C. Progress to Date

Based on the specifications determined in [18], a tactile sensing instrument (TSI) that uses a commercially available pressure pad was developed by the authors. The Industrial TactArray sensor from Pressure Profile Systems (PPS) (Los Angeles, CA) was incorporated into a surgical probe suitable for MIS, Fig. 1. Details of the sensor design can be found in [19]. For the TSI, a custom arrangement of sensing elements is used, consisting of an array with 15 rows and 4 columns of electrodes, resulting in a total of 60 distinct capacitors. In order to address the biocompatibility issues of the probe, a disposable laparoscopic latex sleeve is placed over both the sensor and the shaft of the probe when in use. Details of the sensor and probe can be found in Table I.

Preliminary tests that demonstrate the effectiveness of this hand-held probe, when compared to more traditional tumor localization methods, have been performed with promising results [20].

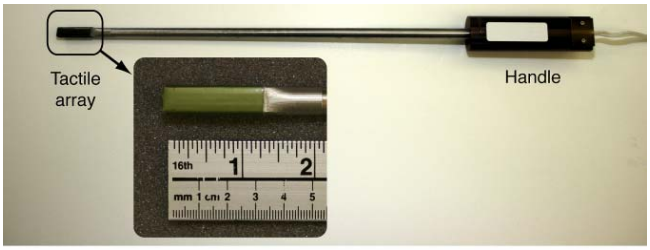

Fig. 1. Tactile sensing instruments.

TABLE I.
DETAILS OF THE TACTILE SENSING INSTRUMENT

Probe shaft length	385 mm
Probe shaft diameter	10 mm
Number of sensor elements	60
Area of each sensor element	4 mm^2
Thickness of sensor	0.3 mm
Pressure range of sensor	0–14,000 kPa
Temperature range of sensor	-40°–200°C

D. Objectives

The objective of this research was to assess the feasibility of using the TSI under robotic control in order to reduce tissue trauma and improve tumor detection. Furthermore, this work aimed to develop an ideal robotic palpation method considering the magnitude of the palpation force, robot motion across the palpated tissue, and a proper visualization technique.

II. EXPERIMENTAL SETUP

Two experimental setups were used to compare human and robot performance when using tactile sensing for tumor localization.

A. Manual Setup

The layout of the manual setup is shown in Fig. 2. The TSI was used to palpate tissue resting on a plate that incorporates a Gamma 6-DOF force/torque sensor (ATI Industrial Automation). To ensure consistency with MIS, the tray and the specimen were shielded by a drape during tissue palpation. A 0˚ scope with a standard resolution camera (Stryker Endoscopy, Inc) was held in place by an endoscopic positioner.

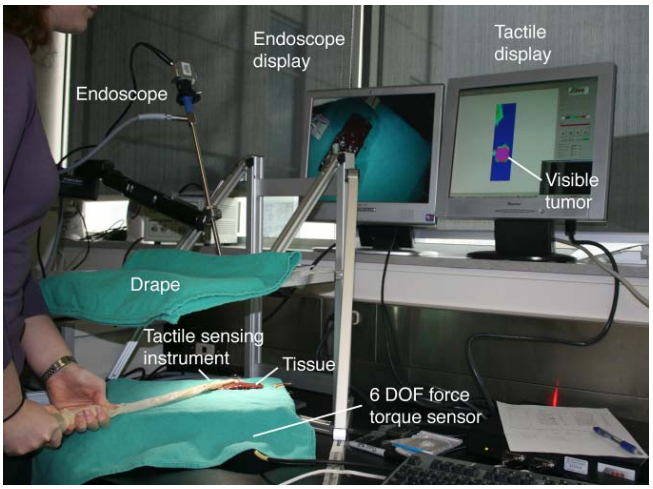

Fig. 2. Layout of the experimental setup for manual testing. The visualization software indicates the presence of a tumor.

The PPS driver and Sapphire® visualization software were used to display the results from the tactile sensor in a meaningful way. The visualization software uses a color spectrum to indicate the levels of localized pressure intensity experienced by the probe, with pink indicating the highest pressure intensity and blue indicating the lowest pressure intensity.

B. Robotic Setup

A 7-DOF Mitsubishi PA10-7C robot was employed to perform robot-assisted force-controlled tissue palpation. In our laboratory, the robot is controlled by a host computer via the ARCNET protocol. The four-layer control architecture consists of the host control computer, motion control card, servo controller and the robotic arm. The host computer communicates with the PA10-7C arm at a sampling rate of 333 Hz. The interaction between the different components of the experimental setup is detailed in Fig. 3.

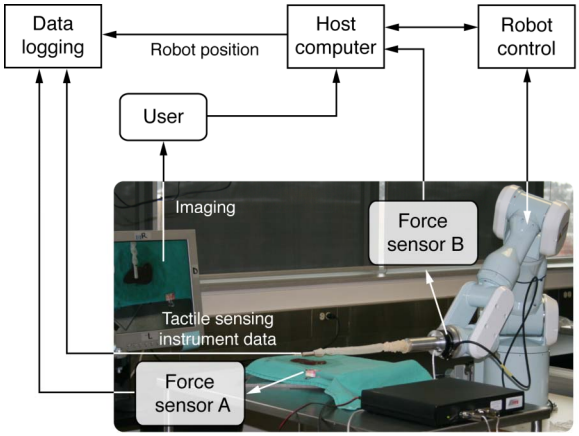

Fig. 3. Configuration of the robotic experimental setup.

C. Robot Control

An Augmented Hybrid Impedance Control (AHIC) scheme has been implemented on the PA10-7C robot to control the palpation force and the position of the end-effector in Cartesian space. The task space in AHIC is divided such that force control is performed in the direction of palpation, while the position and orientation of the end-effector are controlled in the orthogonal directions. The area that is palpated depends on the input provided by the user; however, palpation happens completely autonomously.

In the AHIC scheme [25], there are two control loops. The outer loop takes the desired position and force profiles as inputs and generates the desired Cartesian acceleration that is fed to the inner loop. In the inner loop, the Cartesian acceleration is converted into joint accelerations. The desired link torques are then generated to track the desired position and force profiles (see Fig. 4). The AHIC algorithm consists of three modules, as follows:

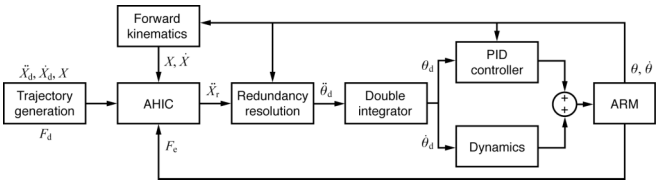

Fig. 4. Flow diagram of the Augmented Hybrid Impedance Control.

1) Augmented Hybrid Impedance Control Module

The AHIC module can be defined as follows:

$$\ddot{X}_t = M_d^{-1}(-F_e + (I-S)F_d - B_d(\dot{X}_t - S\dot{X}_d) - K_d S(X_t - X_d)) + S\ddot{X}_d \quad (1)$$

where F_d is the desired force and F_e is the environment contact force; M_d, B_d and K_d are the desired mass, damping and stiffness parameters; I is the identity matrix; X_t, $\dot{X}_t$ and $\ddot{X}_t$, and X_d, $\dot{X}_d$ and $\ddot{X}_d$ are the target position/orientation, velocity and acceleration, and the desired position/orientation, velocity and acceleration, respectively. S denotes the selection matrix which defines the force and position controlled subspaces. In order to ensure accurate tracking in the presence of model uncertainties, an additional proportional-derivative (PD) loop, is included to minimize the tracking error:

$$\ddot{X}_r = \ddot{X}_t + K_p(X_t - X) + K_v(\dot{X}_t - \dot{X}), \quad (2)$$

where $\ddot{X}_r$ is the reference acceleration, K_p and K_v are the proportional and derivative gains of the PD loop, X and $\dot{X}$ are the Cartesian position/orientation and velocity of the end-effector, respectively.

2) Redundancy Resolution Module

The redundancy resolution module in the inner loop of the AHIC converts the Cartesian acceleration to a desired joint level acceleration and provides it to the joint-based controller. Since the PA10-7C robot has 7 DOFs, the Jacobian is not square. As a result, an additional task is included to lock the redundant joint, thereby making the Jacobian square. A damped least-squares solution at the acceleration level [26] is implemented to damp out the joint velocities in the null-space of the Jacobian as given by the following equation:

$$\ddot{\theta}_d = [J_e^T W_e J_e^T + J_c^T W_c J_c^T + W_v]^{-1} \cdot [J_e^T W_e(\ddot{X}_t - \dot{J}_e\dot{\theta}) + J_c^T W_c(\ddot{Z}) - W_v\lambda\dot{\theta}]^{-1}, \quad (3)$$

where $\ddot{\theta}_d$ is the desired joint acceleration, $\dot{\theta}$ corresponds to the joint velocities, $\ddot{Z}$ is the acceleration corresponding to the secondary task, J_e and J_c are the Jacobian matrices corresponding to the primary and the secondary tasks, W_e and W_c are the corresponding weight matrices, W_v is the singularity robustness factor and λ is the velocity damping factor. The joint accelerations are integrated to obtain the desired joint velocities and angles and fed to the joint control module after canceling the gravity term.

3) Joint Based Controller

Each of the seven joints is controlled to follow a certain desired trajectory. For medical robots, the joint velocities are generally quite small and there is very little change in the configuration of the robot. Due to these assumptions, the joint level controller simplifies to:

$$\tau = \ddot{\theta}_d + K_{pj}(\theta_d - \theta) + K_{dj}(\dot{\theta}_d - \dot{\theta}) + G(\theta), \quad (4)$$

where θ corresponds to the joint angles, θ_d and $\dot{\theta}_d$ are the desired joint angles and velocities, and K_{pj} and K_{dj} are the proportional and derivative gains of the joint level controller. This control strategy was successfully implemented with the robotic setup shown in Fig. 5.

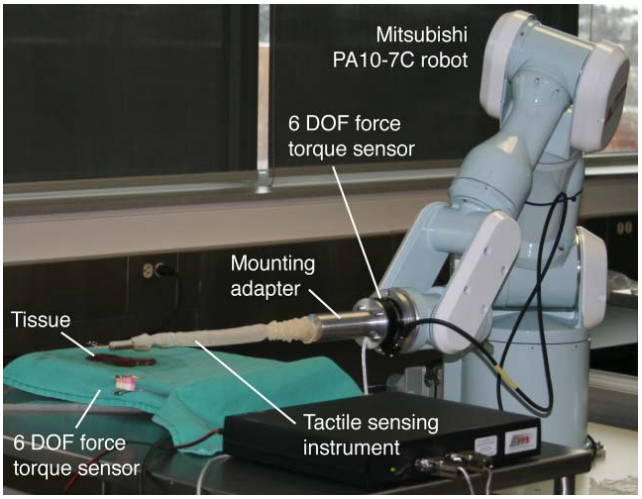

Fig. 5. Robotic setup for palpating tissue.

III. Methods

An experimental evaluation was performed to compare the performance of the Mitsubishi PA10-7C robot to that of human subjects when using tactile sensing for tumor localization.

The tissue used in these experiments was *ex vivo* bovine liver obtained from a local store. To simulate the presence of tumors, 5 mm diameter spherical objects and 10 mm diameter hemispherical objects (see Fig. 6) were pressed into the dorsal side of the liver. These objects were made from thermoplastic adhesive (hot glue) with encased thin metal wires to ensure their visibility in radiographic images, which were later used to assess accuracy.

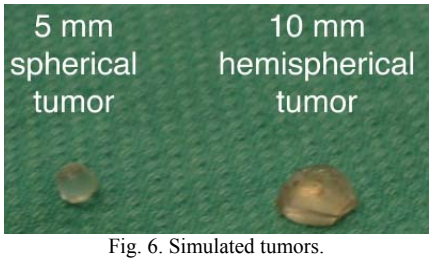

Fig. 6. Simulated tumors.

For each trial, nine *ex vivo* livers were prepared with small tumors and nine with large tumors. Each sample had the possibility of containing zero to two tumors, determined *a priori* through a block randomization process, to which the human subjects were blinded. The performance of each of the methods was assessed using the following measures:

The *success rate* provides a measure of the ability of the sensing method to correctly identify all of the tumors present in each liver sample. The success rate can be determined using four categories [23]: 1) a *true positive test* occurs when the tumor is correctly identified and found in the liver; 2) a *false positive test* occurs when the user indicates that a tumor is found where none is located in that area; 3) a *false negative test* occurs when the user does not find the tumor located in the liver; and 4) a *true negative test* occurs when the user correctly identifies that there is no tumor located in the liver. These four categories can be used to determine measures such as: accuracy (the proportion of tests that were correctly identified as having or not having a tumor); sensitivity (the proportion of tumors present in the samples and test positive); and specificity (the proportion of specimens that do not have tumors and test negative).

The *palpation force* exerted while searching for a tumor is an indication of the potential damage to the tissue. The maximum forces were measured using the ATI Gamma force/torque sensor placed below the specimen.

The *task completion time* is the time required to locate the tumors in the specimen presented during the task. The recorded time begins once the probe has touched the surface of the liver. The task completion time is recorded once the user stops palpating the tissue, signifying the end of the trial.

A. Manual Tests

Four subjects participated in this experiment, two of them with surgical experience. Before the trials, the participants were permitted to practice until comfortable with the TSI, and were informed that any number of tumors could be located in the presented liver (including no tumors). During the trials, the locations of the tumors found by the participants were marked as shown in Fig. 7 (*top*). The time required to place the markers was subtracted from the task completion time, and the force required to insert the pins into the tissue was not recorded. To assess the success rate of the tumor localization method, radiographs of the specimens were taken, Fig. 7 (*bottom*). True positive results were obtained when the marker intersected the tumor in the image. A false negative result was recorded if a tumor was not found. A false positive result was recorded if a marker was noted where there was no tumor present. A true negative test was recorded when the subject found no tumors and the specimen contained no tumors.

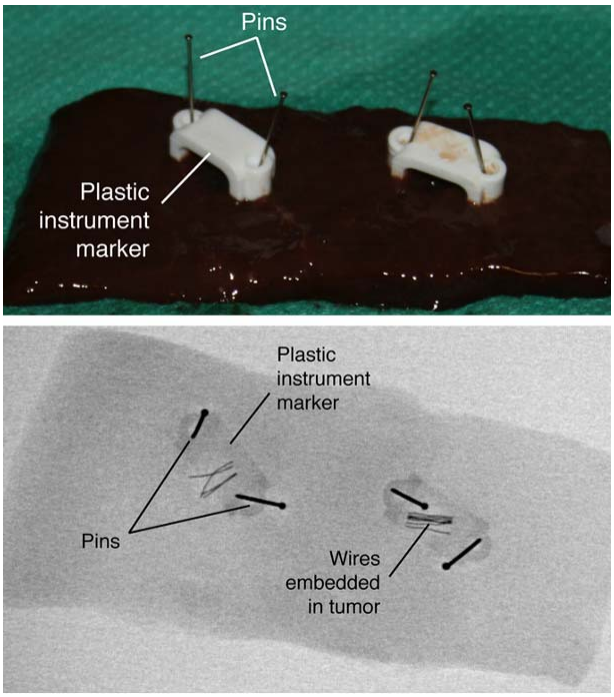

Fig. 7. Manually palpated tissue with suspected tumor sites marked by a plastic marker held in place with two pins (*top*). Radiograph of tissue, 10 mm tumors with embedded wire and plastic instrument markers (*bottom*).

B. *Robotic Tests*

In the robotic setup, the robot approaches the tissue under force control until the wrist force sensor (a second 6-DOF ATI Gamma) registers a desired force. Instantaneously, the readings from the TSI are recorded to register the force profile of the contact made with the tissue. The robot is then commanded to move up and sideways in 3 mm steps through position control to the next point. This process continues until all of the desired points specified by the user have been palpated. Preliminary tests showed that a 4 N palpation force was adequate to obtain consistent results.

A custom-designed software program was created to record the position of the robot, the force exerted on the tissue by the robot (as measured below the specimen), and the corresponding pressure map of the TSI. During post-processing of the experimental data, a graphical representation of position versus pressure was generated. This graph serves to indicate the tumors located by the robot, presented as a color map with red indicating the highest pressures and blue indicating the lowest pressures applied on the TSI. The assessment of these plots was performed by four volunteers who were blinded to the number of tumors present in each trial. A similar assessment of success rate was performed and compared to that of the human subjects.

The Statistical Package for Social Sciences (SPSS, Chicago, IL) software, version 15.0 for Windows, was used for statistical analysis. A one-way analysis of variance (ANOVA) was performed to establish differences among the different methods. The Dunnett test was then performed to determine significant differences between the individual groups. Unpaired *t*-tests were used to determine differences between the large and the small tumors within each group.

IV. Results

The effectiveness of the robot control system on the PA10-7C is shown in Fig. 8. This figure shows (*top*) that the robot approaches the tissue under force control and consequently does not follow the desired Cartesian trajectory. Once the force of palpation reaches the desired force (*bottom*), the robot is commanded to move to the next point under position control. The switching between force and position control is highlighted in the time interval from 25.8 seconds to 29.4 seconds (*top*).

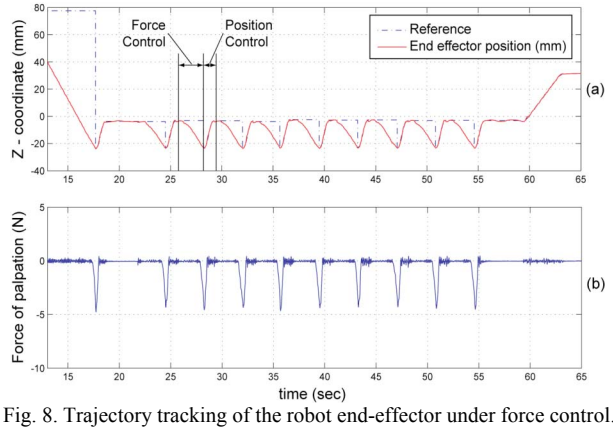

Fig. 8. Trajectory tracking of the robot end-effector under force control.

Fig. 9 shows sample graphs of the pressure maps obtained when the robot palpated the tissue. A Fleiss' kappa of 0.89 shows that the degree of agreement among the assessors of the pressure maps is in the "almost perfect agreement" range.

The results of force and time are shown in Table II. These results show that there is a significant difference in the forces applied by the humans in comparison to the robotic method. The application of forces greater than 6 N for extended periods of time caused visible damage to the tissue. It was found that in the human trials, the applied forces exceeded 6 N for 7% of the time.

Table III shows the measures of accuracy typically used to assess the effectiveness of a diagnostic test. This analysis was performed as a way of assessing the effectiveness of the TSI for the determination of tumor presence, and shows a significant improvement in all of the measures when using robotic assistance to control the motion of the instrument.

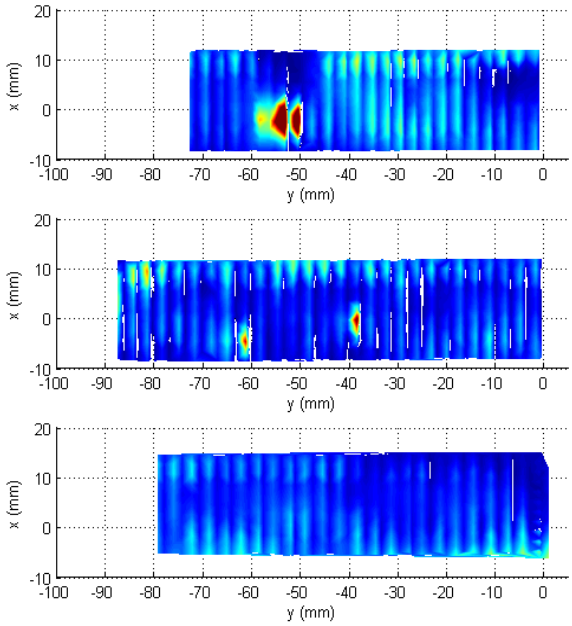

Fig. 9. Sample pressure maps for the robot palpation experiments: one large tumor (*top*), two small tumors (*middle*) and no tumors (*bottom*).

TABLE II.
RESULTS FOR FORCE AND TIME

	Maximum Force (N)	Average Time (s)
Human		
Small Tumors	8.14 ± 2.9	217.5 ± 126.2
Large Tumors	8.12 ± 3.6	176.8 ± 124.9
Average	8.13 ± 3.2	197.2 ± 126.4
Robot		
Small Tumors	4.96 ± 0.1	129.8 ± 25.0
Large Tumors	5.38 ± 0.9	156.0 ± 33.2
Average	5.17 ± 0.6	142.9 ± 31.5

TABLE III.
PERFORMANCE MEASURES FOR THE TACTILE SENSING INSTRUMENT

Trial	Accuracy	Sensitivity	Specificity
Human			
Small Tumors	49%	67%	22%
Large Tumors	69%	94%	30%
Average	59%	81%	26%
Robot			
Small Tumors	87%	92%	75%
Large Tumors	98%	97%	100%
Average	92%	94%	86%

V. Discussion and Conclusions

The results of this study show that using a tactile sensing instrument under robotic control reduces the maximum force applied to the tissue by more than 35% when compared to manual manipulation of the instrument. Detection accuracy is increased from 59% under manual manipulation of the instrument to 92% under robotic control. Thus, the use of robotic assistance for tactile sensing during MIS is not only feasible, but results in reduced tissue trauma and increased tumor detection compared to the manual manipulation of a tactile sensing instrument. For more details on the effect of different control methods see [24].

It must be noted that while the robot only performed the palpation for offline analysis of the data, the humans were simultaneously assessing the information. Therefore, the average task completion time between the humans and the robot cannot be compared and is shown only as reference.

The difference between robot and human tissue palpation is that the robot can apply a consistent amount of force at each step and can move systematically over the entire surface of the tissue, thereby producing a complete, continuous map of the entire surface. A force of 4 N was found to be the ideal force required to obtain consistent results when trying to locate 5 mm and 10 mm tumors. This is consistent with a similar study performed by the authors, in which it was found that the average maximum force applied by surgeons manually palpating tissue was 4.4 N.

As expected, both the human and robotic methods performed better when detecting 10 mm tumors than when detecting 5 mm tumors. It should be noted that, the "large" tumors used in this study are not clinically large. In fact, most diagnostic tests are not capable of detecting tumors that are smaller than 10 mm [25]. The smaller 5 mm tumors were included in this study to properly assess the improvement of one method over another under the worst case scenario.

It should be noted that this system is not at a stage in which it can be used clinically. The robotic system used is an industrial robot that is not safe to operate in close proximity to humans and the motion of the instrument is not designed to mimic the remote center of motion required for MIS.

Future work involves incorporating a virtual remote center of motion into the robot controls. A TSI with an articulating head will be developed for these experiments. Furthermore, the feasibility of combining tactile and kinesthetic feedback for tumor localization will be assessed.

Acknowledgment

The authors would like to thank Greig McCreery, Dave Bottoni, Adam Katchky and the CSTAR staff for their help with the experimental evaluation.

References

[1] American Cancer Society. 2007. Cancer Facts and Figures 2007. No. 500807. Atlanta, GA. American Cancer Society Inc. www.cancer.org.

[2] J. Dargahi and S. Najarian, "An integrated force-position tactile sensor for improving diagnostic and therapeutic endoscopic surgery," *Bio-Med Mater. Eng*, vol. 14, no. 2, pp. 151–166, 2004.

[3] M.V. Ottermo, *et al*., "The role of tactile feedback in laparoscopic surgery," *Surg. Laparosc. Endosc. Percutan. Tech*, vol. 16, no. 6, pp. 390–400, 2006.

[4] J. Rosen and B. Hannaford, "Markov modeling of minimally invasive surgery based on tool/tissue interaction and force/torque signatures for evaluating surgical skills," *IEEE T Bio-Med Eng*, vol. 48, no. 5. pp. 579–591, 2001.

[5] G. Tholey, A. Pillarisetti, W. Green, and J.P. Desai, "Design, development, and testing of an automated laparoscopic grasper with 3-D force measurement capability," In *Proc. Int. Conf. Noise and Vibration Engineering*, Leuven, Belgium, 2004, pp. 38–48.

[6] F. Van Meer, D. Esteve, A. Giraud, and A.M. Gué, "Si-micromachined 2D force sensor for a laparoscopic instrument," *Int. Conf. Computer Assisted Radiology and Surgery*, International Congress Series, vol. 1268, Chicago, Illinois, 2004, pp. 1334.

[7] S. Shimachi, Y. Fujiwara, and Y. Hakozaki, "New sensing method of force acting on instrument for laparoscopic robot surgery," *Int. Conf. Computer Assisted Radiology and Surgery (CARS)*, International Congress Series Vol. 1268, Chicago, Illinois, pp. 775–780, 2004.

[8] P. Dubois, "In vivo measurement of surgical gestures," *IEEE T Bio-Med Eng*, vol. 49, no. 1, pp. 49–54, 2002.

[9] P.J. Berkelman, L.L. Whitcomb, R.H. Taylor, and P. Jensen, "A miniature microsurgical instrument tip force sensor for enhanced force feedback during robot-assisted manipulation," *IEEE T Robotic Autom*, vol. 19, no. 5, pp. 917–922, 2003.

[10] S. Schostek, C.-N. Ho, D. Kalanovic, and M.O. Schurr, "Artificial tactile sensing in minimally invasive surgery—a new technical approach," *Minim Invasiv Ther*, vol. 15, no. 5, pp. 296–304, 2006.

[11] P.S. Wellman and R.D. Howe, "Extracting Features From Tactile Maps," In *Proc. Int. Conf. Medical Image Computing and Computer-Assisted Intervention*, Cambridge, UK, 1999, pp. 1133–1142.

[12] R.A. Beasley and R.D. Howe, "Tactile tracking of arteries in robotic surgery," In *Proc. IEEE Int. Conf. Robotics and Automation*, vol. 4, Washington, DC, 2002, pp. 3801–3806.

[13] A.P. Miller, W.J. Peine, J.S. Son, and Z.T. Hammoud, "Tactile imaging system for localizing lung nodules during video assisted thoracoscopic surgery," *IEEE Int. Conf. Robotics and Automation,* Rome, Italy, 2007, pp. 2996–3001.

[14] J. Rosen and B. Hannaford, "Force controlled and teleoperated endoscopic grasper for minimally invasive surgery—experimental performance evaluation," *IEEE T Bio-Med Eng*, vol. 46, no. 10, pp. 1212–1221, 1999.

[15] M. Tavakoli, R.V. Patel, and M. Moallem, "Haptic interaction in robot-assisted endoscopic surgery: a sensorized end-effector," *Int J Med Robot Comp*, vol. 1, no. 2, pp. 53–63, 2005.

[16] P. Dario and M. Bergamasco, "An advanced robot system for automated diagnostic tasks through palpation," *IEEE T Bio-Med Eng*, vol. 35, no. 2, pp.118–126, 1988.

[17] R.L. Feller, C.K.L. Lau, C.R. Wagner, C.P. Perrin, and R.D. Howe, "The effect of force feedback on remote palpation," In *Proc. IEEE Int. Conf. Robotics and Automation*, New Orleans, Louisiana, 2004, pp. 782–788.

[18] G.L. McCreery, A.L. Trejos, R.V. Patel, M.D. Naish, and R.A. Malthaner, "Feasibility of locating tumours in lung via kinesthetic feedback," *Int J Med Robot Comp*, vol. 4, no. 1, pp. 58–68, 2008.

[19] W.J. Peine, J.S. Son, and R.D. Howe, "A palpation system for artery localization in laparoscopic surgery," *Symposium on Medical Robotics and Computer Assisted Surgery*, Pittsburgh, USA, 1994.

[20] M.T. Perri, *et al*., "A new tactile imaging device to aid with localizing lung tumours during thoracoscopic surgery," In *Proc. Int. Conf. Computer Assisted Radiology and Surgery (CARS)*, 22nd International Congress Series, Barcelona, Spain, 2008.

[21] R.V. Patel, H.A. Talebi, J. Jayender, and F. Shadpey, "A robust position and force control strategy for 7-DOF redundant manipulators," *IEEE-ASME T Mech*, under review, 2008.

[22] R.V. Patel and F. Shadpey "Control of redundant robot manipulators: theory and experiments," *Lecture Notes in Control and Information Sciences*, vol. 315, Springer-Verlag, Heidelberg, Germany, 2005.

[23] M. Davidson, "The interpretation of diagnostic tests: a primer for physiotherapists," *Aust J Physiother*, vol. 48, pp. 227–232, 2002.

[24] A.L. Trejos, J. Jayender, M.T. Perri, M.D. Naish, R.V. Patel, and R.A. Malthaner, "Robot-assisted tactile sensing for minimally invasive tumor localization," *The International Journal of Robotics Research – Special Issue on Medical Robotics*, under review, August 2008.

[25] P. Singh, *et al.*, "EUS for detection of the hepatocellular carcinoma: results of a prospective study," *Gastrointest Endosc*, vol. 66, no. 2, pp. 265–273, 2007.